Meson-exchange enhancement of the first-forbidden $^{96}Y^{g}(0^{-}) \rightarrow {}^{96}Zr^{g}(0^{+})$ β transition: β decay of the low-spin isomer of ^{96}Y

H. Mach*
Clark University, Worcester, Massachusetts 01610

E. K. Warburton†
Universität Heidelberg and the Max-Planck-Institut für Kernphysik, Heidelberg, Federal Republic of Germany

R. L. Gill and R. F. Casten
Brookhaven National Laboratory, Upton, New York 11973

J. A. Becker
Lawrence Livermore National Laboratory, Livermore, California 94550

B. A. Brown
Cyclotron Laboratory and Department of Physics and Astronomy, Michigan State University, East Lansing, Michigan 48824

J. A. Winger
Ames Laboratory, Iowa State University, Ames, Iowa 50011
(Received 13 June 1989)

We have investigated the 0^{-} $^{96}Y^{g}$ β decay to the levels of ^{96}Zr. A detailed decay scheme comprised of 63 γ rays and 44 energy levels has been obtained from γ singles, γ multispectral scaling, and γ-γ and $E0$-γ coincidences. Q_{β} was measured using the β-γ coincidence technique, while absolute $E0$ and γ-ray intensities were obtained from singles conversion electron and γ-ray spectra measured at beam saturation. The high sensitivity of the study was aimed at investigating the β feeding of levels with excitation enegy above 4 MeV. Although most of the new levels were found in this region, their total β feeding was found to be below 0.6%. The first-forbidden β-decay rate for 0^{-} $^{96}Y^{g} \rightarrow 0^{+}$ $^{96}Zr^{g}$ has been calculated within the framework of the spherical shell model using a model space of $\pi(0f_{7/2}, 0f_{5/2}, 1p_{3/2}, 1p_{1/2}, 0g_{9/2})\nu(0g_{7/2}, 1d_{5/2}, 1d_{3/2}, 2s_{1/2})$ with limitations on the orbit occupancies. Additional evidence for meson enhancement of the timelike component of the axial current is obtained; the meson-exchange enhancement factor was found to be 1.75 ± 0.30, where the uncertainty arises from the calculation.

I. INTRODUCTION

Weak interaction processes in nuclei normally can be assumed to arise solely from nucleonic degrees of freedom. Kubodera, Delorme, and Rho[1] first suggested that pion exchange, particularly one-pion exchange, should have a large effect on the rank-zero timelike component of the axial current, A_0. Since then, there has been considerable interest in the contribution of the meson-exchange-current (mec) to this operator because it affords a unique opportunity to test our understanding of the interplay of pions and nucleons in nuclei.[2-5] The ideal process for the study of A_0 is $0^{-} \leftrightarrow 0^{+}$ beta decay[1-13] since in this process only rank-zero matrix elements of the timelike and spacelike components of the axial current contribute.

Fast $0^{-} \rightarrow 0^{+}$ first-forbidden β transitions have been studied in the vicinity of doubly closed-shell nuclei such as ^{16}O (Refs. 4–13), ^{96}Zr (Refs. 8 and 14), and ^{208}Pb (Ref. 8). In these transitions, the dominant component arises from a $s_{1/2} \leftrightarrow p_{1/2}$ transition. The relative purity of the shell-model configurations and the aforementioned meson-exchange effects provide enhancement of the decay rates over empirical limits[15] for first-forbidden decays.

The enhancement has been studied from two points of view. The more fundamental studies address the direct calculation of the pion exchange. Procedures and results are reviewed by Towner[11] and Kirchbach.[4,5,8] There are large uncertainties in these difficult calculations. Thus another approach is desirable. Namely, to extract the magnitude of the meson enhancement by a comparison between impulse approximation calculations and experiment.[9,10] This is the procedure followed in this present study.

$^{16}N(0^{-}) \rightarrow {}^{16}O(0^{+})$ decay is the best studied case.[4-11] Although the shell-model calculations which have been done strongly imply meson enhancement, the uncertain-

ties involved do not rule out the absence of meson enhancement with the desired certainty. In any case, the magnitude of the enhancement is poorly determined. It is very difficult—if not impossible—to refine the shell-model calculations much further in this or other cases. Thus, the best we can do is to examine as many rank-zero decays as possible. If the uncertainties in the calculations are of somewhat different natures in the different cases and an omnibus comparison shows the need for meson enhancement, then our confidence in the extracted enhancement will be correspondingly higher. Such an omnibus comparison has been made for the $A=16$ region[9,10] but it is desirable to expand the comparison to other regions of A where the determination of the extent of meson enhancement has a different dependence on the underlying nuclear structure.[16]

In general, the stronger the rank-zero decay, the more accurate the shell-model calculation. This is so because almost all other terms interfere destructively with the dominant $s_{1/2}\leftrightarrow p_{1/2}$ component. The $\log f_0 t$ of 5.53 for $^{16}\mathrm{N}(0^-)\rightarrow{}^{16}\mathrm{O}(0^+)$ corresponds to a decay strength, $B_1^{(0)}$, which is 46% of the $A=16$, $\nu 1s_{1/2}\rightarrow\pi 0p_{1/2}$ single-particle unit defined by Warburton, *et al.*[17] The $^{96}\mathrm{Y}(0^-)\rightarrow{}^{96}\mathrm{Zr}(0^+)$ $\log f_0 t$ value of 5.61 (Ref. 14) corresponds to 52% of a similar $A=96$, $\nu 2s_{1/2}\rightarrow\pi 1p_{1/2}$ single-particle unit. It is clear that $^{96}\mathrm{Y}^g$ decay provides a particularly suitable environment for the study of the meson-exchange contribution to A_0.

On the experimental side, however, the decay of $^{96}\mathrm{Y}^g\rightarrow{}^{96}\mathrm{Zr}^g$ has been a subject of controversy.[14] In the study of Sadler *et al.*[18] the decay of the 0^- ^{96}Y ground state was observed to populate only one excited state, the 0_2^+ state which they located at 1594 keV and which decays to the 0_1^+ ground state by an $E0$ transition. They reported β-feeding intensities of 5% and 95% to the 0_2^+ and 0_1^+ states, respectively. In subsequent studies, summarized by Mueller,[19] the feeding of the 0_2^+ state was found to be 25%. More sensitive measurements,[14] performed recently at the TRISTAN mass separator at Brookhaven National Laboratory (BNL), corrected a number of inaccuracies in earlier works and revealed a substantially different decay scheme which involved eight excited states and thirteen γ transitions. The dominant β branch was found to feed 0_1^+ with 95% of the intensity, while the β intensity to 0_2^+ was found to be only 1.3%, a number much lower than previously reported.[18,19] Furthermore, the excitation energy of the 0_2^+ state was determined to be 1581.4(5) keV.

A tacit assumption made in those studies was that no substantial β feeding goes to levels above 4 MeV in excitation. In particular, due to the limited scope of the study by Mach *et al.*,[14] no information was obtained on γ transitions with $E_\gamma > 4.2$ MeV. However, in a recent parallel study[20] on the $A=98$ mass chain, absolute γ intensities were found to be higher than the previously adopted values by a factor of ~ 4. As a consequence, in the decay of $^{98}\mathrm{Y}^g$—which in many respects parallels the decay of $^{96}\mathrm{Y}^g$—almost 50% of the β feeding was found to populate two levels in ^{98}Zr at about 4.3 MeV in excitation. In view of these developments, a new investigation of the decay of $^{96}\mathrm{Y}^g$ with a particular emphasis on the high-energy γ transitions and on independent methods of extracting absolute intensities for the $E0$ and γ transitions is called for in order to establish a reliable picture of the decay necessary for a comparison to the model calculations.

To summarize, in this work we report results of a detailed experimental study of the 5.4 s 0^- $^{96}\mathrm{Y}^g$ decay, combined with the results of calculations obtained within the framework of the spherical shell model. Brief reports on some aspects of our results have already been published.[21,22]

II. EXPERIMENTAL PROCEDURES

A. Measurements

The measurements were performed at the TRISTAN mass separator online to the High Flux Beam Reactor at Brookhaven National Laboratory. ^{96}Rb activity was produced by thermal neutron fission of an enriched ^{235}U target inside the separator's thermal ion source.[23] The temperature of the source was kept at its operational minimum; a step necessary to suppress direct production of ^{96}Sr and ^{96}Y ions. Consequently, the low-spin isomer of ^{96}Y was populated from the decay chain $^{96}\mathrm{Rb}(t_{1/2}=0.2$ s$)\rightarrow{}^{96}\mathrm{Sr}(t_{1/2}=1.0$ s$)\rightarrow{}^{96}\mathrm{Y}(t_{1/2}=5.4$ s$)\rightarrow{}^{96}$Zr. The mass separated ^{96}Rb beam was deposited onto a movable, aluminized Mylar tape. Detectors were assembled either at the "parent port," to view directly the point of beam deposition, or at the "daughter port": a shielded counting station about 50 cm away. With the exception of the saturated beam measurements, all the measurements were performed in the daughter port configuration. The cycle time sequence was designed to maximize the yield of yttrium activity at the daughter port. In such a cycle, the source was accumulated at the parent port for a period of time, T_1, then the beam was electrostatically deflected for a time interval, T_2, to allow the short-lived ^{96}Rb and ^{96}Sr activity to decay. Afterward, the source was moved on the tape to the daughter port where the counting of the radioactive sample took place over a period of time T_1+T_2, while a new source was prepared at the parent port. The cycle times of $T_1=8.0$ s and $T_2=8.0$ s were used for the γ singles, γ-multispectral scaling (GMS), and γ-γ coincidence measurements, while $T_1=1.2$ s and $T_2=8.0$ s were used for the Q_β measurements.

B. High-energy gamma-ray measurements

The γ-ray measurements, which consisted of γ singles, GMS, and γ-γ-t coincidences, were optimized to search for high-energy γ transitions in the energy range above 3 MeV. Besides the advantage of higher statistics collected over a longer period of time, we have used two additional features which enhanced our sensitivity over the previous TRISTAN measurements[14] by almost a factor of 50. First, larger volume ($\epsilon=26\%$) Ge detectors were used, and second, thick Al shielding around the radioactive sample almost eliminated that portion of the background

which would have come from energetic β rays recorded in the Ge detector.

Figure 1 presents a partial high-energy γ spectrum. The γ lines arise mainly from the decay of $^{96}Y^{g}$ and ^{95}Sr ($t_{1/2}=25$ s), the latter populated from a strong,[19] 13.8(9)%, β-delayed neutron branch of ^{96}Rb. Energies of the new transitions were determined from internal calibrations using known[14,19,24] transitions from the decay of ^{96}Sr, ^{96}Y, ^{95}Sr, and from known high-energy neutron-capture lines. Detector efficiency calibrations were performed offline using standard sources and extrapolated to the high-energy region (3–10 MeV) with the help of Monte Carlo efficiency calculations[25,26] for the detector size and geometry used in the measurements. For the extrapolated region, we assigned a conservative uncertainty increasing with energy from 10% at 2.5 MeV to 15% at 5 MeV.

The assignment of γ transitions to the decay of $^{96}Y^{g}$ is based exclusively on the GMS results with the exception of a few weaker lines for which the assignments are based on coincidence relations with strong γ rays in the decay.

TABLE I. Comparison of half-lives measured in this work and in previous studies. All values are in seconds.

Nucleus	Half-life		
	This Work[a]	Ref. 14	Refs. 19 and 24
^{96}Y	5.34(5)	5.4(1)	6.2(2)[b]
^{96}Sr	1.07(1)	1.04(1)	1.06(3)
^{95}Sr	26.0(9)		25.1(2)

[a]Obtained from fitting the GMS-decay curve for the 1750-, 809-, and 686-keV γ rays from the decay of ^{96}Y, ^{96}Sr, and ^{95}Sr, respectively.

[b]Obtained from fitting a β-decay curve; the longer lifetime is possibly due to admixture of the 10-s isomer of ^{96}Y.

In the GMS cycle time of 16 s, 32 consecutive spectra were collected. The decay curve for each transition was normalized to a pulser spectrum and fitted to a single-component decay to extract the half-life of its dominant component. It was then fitted to a two-component decay with fixed half-lives of 5.34 and 25.1 s for each decay in

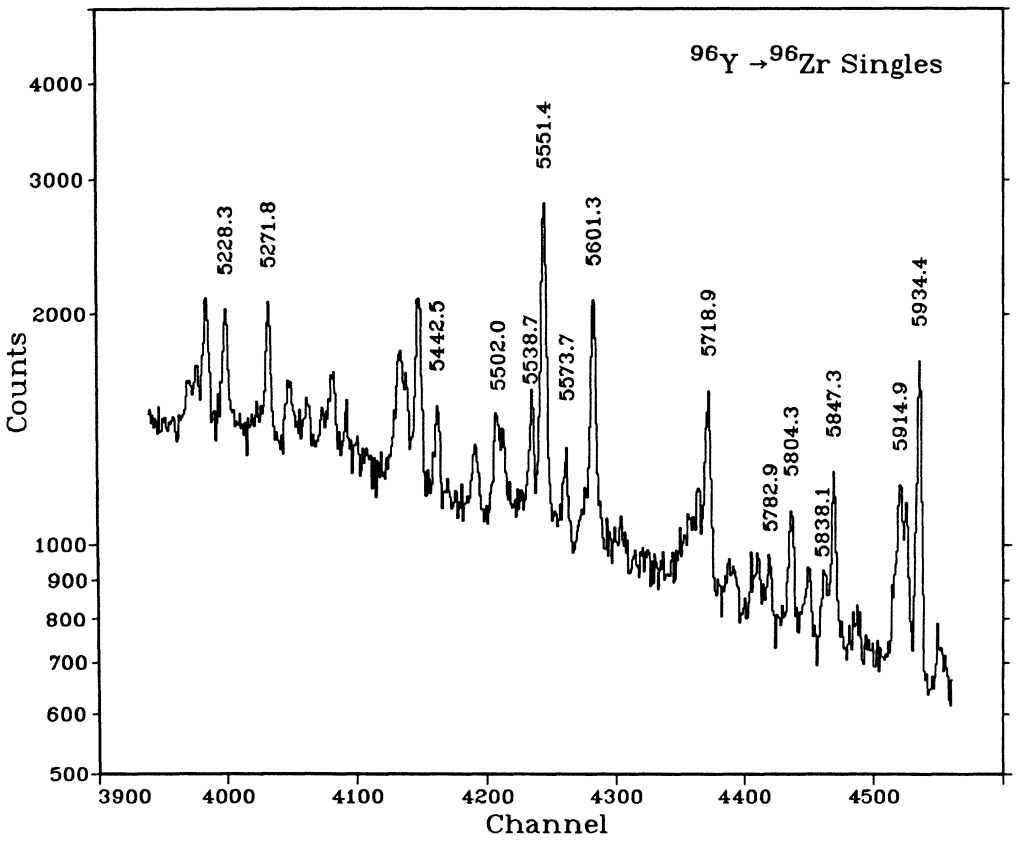

FIG. 1. A portion of a high-energy γ-ray singles spectrum, Transitions in ^{96}Zr populated from the decay of 5.4 s $^{96}Y^{g}$ are marked by their energies in keV; the other transitions are impurity lines from the decay of ^{95}Sr and from the general reactor background. The 5551-keV transition, with an intensity 1.9% of the 1750-keV $2_1^+ \rightarrow 0_1^+$ transition, is the most intense transition observed in the $E_\gamma > 1200$-keV region.

TABLE II. Energies, intensities, GMS, and coincidence results for γ rays in the decay of the 5.34-s isomer of ^{96}Y. Uncertain values or assignments are enclosed in square brackets.

E_γ (keV)	I_γ^a	Assignment (keV)	GMS	Coincidences (keV)
146.653(10)[b]	32(2)	1897.1→1750.4	*c*	329, 469, 772, 781, 1315, 1612, 1626, 1750, 2940
328.7(2)[b]	22.1(8)	2225.7→1897.1	*c*	147, 469, 700, 1750, 1897
469.5(2)[b]	73(2)	2695.2→2225.7	*c*	147, 329, 475, 644, 1750, 1897, 2225, *E*0
475.3(2)[b]	80(3)	2225.7→1750.4	*c*	469, 700, 1750
644.4(2)[b]	30(1)	2225.7→1581.4	*c*	469, 700, 1225, *E*0
699.9(3)	7.6(6)	2925.5→2225.7	*c*	147, 329, 475, 644, 1332, 1750, 1912, 2226, *E*0
771.7(2)[b]	6.4(10)[d]	2668.9→1897.1	*c*	147, 781, 1750, 1897
781.2(2)[b]	20(3)	3450.3→2668.9	*c*	147, 772, 918, 1750
918.5(2)[b]	32(2)	2668.9→1750.4	*c*	[256], 781, 1750
1175.0(3)[d]	19(2)[d]	2925.5→1750.4	*e*	1332, 1750, 1912
1225.2(5)[d]	2.4(10)[d]	3450.3→2225.7	*e*	2226, *f*
1315.0(3)[d]	3.3(4)[d]	3213.3→1897.1		147, 1626, 1750
1332.4(4)[d]	5.5(10)[d]	4257.9→2925.5	*e*	700, 1175
1462.0(4)[d]	2.9(7)[d]	3212.3→1750.4	*e*	1750
1612.1(4)[d]	0.8(4)[d]	3509.2→1897.1	*e*	147
1625.8(4)[d]	10(3)	4837.8→3212.3	*c*	147, 1315, 1750, 3213, *f*
1699.6(4)[d]	12(3)	3450.3→1750.4	*c*	1750
1750.4(2)[b]	1000(3)	1750.4→0.0	*c*	147, 329, 469, 475, 700, 772, 781, 918, 1175, 1315, 1462, 1626, 1700, 1912, [1956], 2940, [2274], 3087, 4163
1897.4(4)	6(2)	1897.1→0.0	*c*	329, 772
1912.1(4)[d]	3.5(8)[d]	4837.8→2925.5	*e*	700, 1175, 1750, *f*
[1956.3(10)][d,g]	1.5(5)[d]	[4881.8→2925.5]	*c*	[1174, 1750], *f*
2225.6(4)[b]	137(8)	2225.7→0.0	*c*	469, 700, 1225
[2274.0(8)][d,g]	2.2(8)[d]	[4024.4→1750.4]	*e*	[1750]
2940.0(4)[d]	6.0(15)[d]	4837.8→1897.1		147, 1750, 1897
3086.9(7)[d]	4.5(7)	4837.8→1750.4	*c*	1750, *f*
3212.9(7)[d]	2.9(16)	3212.3→0.0	*	1626
3257.4(7)	3.6(8)	4837.8→1581.4	*	*E*0, *f*
[3615.2(10)][d,g]	1.4(6)[d]	[5196.6→1581.4]	*e*	[*E*0]
3701.0(10)	5.0(10)[h]	[3701.0→0.0]	*c*	*h*
3730.8(7)	6.2(7)	5312.2→1581.4	*c*	*E*0
3826.6(7)	5.6(7)[h]	5408.0→1581.4	*	*E*0[h]
3861.7(6)	12.0(13)[h]	5442.8→1581.4	*c*	*E*0[h]
3992.2(8)	1.9(5)	5573.6→1581.4	*	[*E*0]
4044.2(10)	1.7(5)	5625.6→1581.4		*E*0
[4071.2(10)][d,g]	1.4(5)[d]	5652.6→1581.4	*e*	[*E*0]
4119.6(6)	4.4(5)	5701.0→1581.4	*e*	*E*0
[4159.8(10)][g]	0.9(4)	[5741.2→1581.4]	*	[*E*0]
4162.9(10)[d]	5.8(11)	5914.5→1750.4	*c*	1750
[4334.2(15)][g]	1.1(3)	[5914.5→1581.4]	*	[*E*0]
4512.4(7)	4.7(9)[h]	4512.4→0.0	*c*	*h*
[4562.7(10)][g]	0.9(4)	[6143.3→1581.4]	*	[*E*0]
4737.4(8)	4.5(8)	4737.4→0.0	*c*	
4839.2(8)	10.1(19)	4837.8→0.0	*c*	NC
4895.1(7)	13.4(22)[h]	4895.1→0.0	*e*	*h*
4914.0(10)	3.9(20)[h]	[4914.0→0.0]	*c*	*h*
4929.0(9)	9.4(16)	4920.0→0.0	*c*	NC
5228.3(6)	5.5(9)	5228.3→0.0	*c*	NC
5271.8(6)	6.1(9)	5271.8→0.0	*c*	
5442.5(7)	4.3(6)[h]	5442.8→0.0	*c*	*h*
[5502.0(8)][g]	5.2(8)	[5502.0→0.0]	*	
5538.7(6)	4.5(7)	5538.7→0.0	*c*	
5551.4(6)	19.0(24)	5551.4→0.0	*c*	NC
5573.7(8)	2.6(5)	5573.6→0.0	*c*	

TABLE II. (*Continued*).

E_γ (keV)	I_γ^a	Assignment (keV)	GMS	Coincidences (keV)
5601.3(6)	14.4(18)	5601.3→0.0	*c*	NC
5718.9(8)	10.3(13)	5718.9→0.0	*c*	
5782.9(8)	1.6(4)	5782.9→0.0	*c*	
5804.3(7)	3.8(6)	5804.3→0.0	*c*	
5838.1(10)	2.7(6)	5838.1→0.0	*c*	
5847.3(6)	6.3(10)	5847.3→0.0	*c*	
5914.9(8)	5.6(10)	5914.5→0.0	*c*	
5934.4(6)	12.2(15)	5934.4→0.0	*c*	
6141.6(14)	1.5(5)	6143.3→0.0	*c*	
6231.4(11)	3.5(6)	6231.4→0.0	*c*	

[a]Multiply by 0.00235(24) to obtain I_γ per 100 decays of ^{96}Y.
[b]Energies from Ref. 14.
[c]GMS data consistent with the 5.3-s half-life.
[d]Energies or intensities deduced from γ-γ or $E0$-γ coincidences.
[e]GNS results indicate mixing of the ^{96}Zr line with an impurity line.
[f]Coincidence results indicate some mixing with a transition from the ^{95}Sr→^{95}Y decay.
[g]Association of this transition with ^{96}Zr is probable but not certain.
[h]Mixed with a first or second escape peak from transitions of higher energy (a broadened 511-keV line was present in the coincidence spectrum); intensity of the impurity line was subtracted.
*GMS results of poor quality.
[NC]No coincident transitions were observed.

order to test the possibility of a second component in a full-energy peak that could arise from a competing decay. This approach was dictated by the high density of the transitions and the fact that portions of the spectrum are dominated by strong transitions from the ^{95}Sr decay ($t_{1/2}=25.1$ s) that could have masked weaker lines from ^{96}Y ($t_{1/2}=5.3$ s). The half-lives deduced from the strongest transition in each decay are presented in Table I. The half-lives represent an average result obtained from the analysis of several consecutive data sets collected during the run, each with statistics increased over the previous set. This was done to minimize systematic effects potentially induced by a deadtime correction procedure in which the number of counts in a full energy peak was normalized to the number of pulser counts accepted in the same spectrum. That is, a small systematic effect could arise from the fact that the γ flux fluctuates over the time of the measurement. No meaningful differences were observed between results from different data sets. The half-lives of ^{96}Sr and ^{95}Sr provide a useful check on the normalization procedures since the first is significantly shorter while the second is longer than the half-life under consideration. One should note that the agreement for the ^{95}Sr half-life is particularly encouraging in view of the fact that the GMS cycle time of 16 s was short in comparison to the half-life of ~25 s and thus limited the quality of the fit. The ^{96}Y half-life adopted in the most recent $A=96$ compilation[19] is significantly longer than in both TRISTAN measurements, and probably resulted from the difficulty of the previous measurements in separating the two isomeric decays of ^{96}Y which have comparable half-lives of 5.4 and 9.6 s, respectively.[19] As in the early measurement,[14] we do not observe in our spectra any trace of γ rays from the 9.6-s high-spin isomer of ^{96}Y. The energies and intensities of the transitions assigned to the decay of the 5.4 s isomer of ^{96}Y are listed in Table II.

In the γ-γ-t measurements, about 5.5×10^7 coincidence events were stored, in event mode, on magnetic tapes and sorted offline. The observed coincidence relations are listed in the last column of Table II. Clear and definite evidence in the coincidence spectrum for the previously unobserved 1699-keV line indicates the greatly enhanced sensitivity over the previous TRISTAN measurements (Ref. 14). No transitions were observed in the γ-γ coincidences with $E_\gamma>4.2$ MeV.

C. Q_β measurements

The Q_β values for the decay of ^{95,96}Sr and ^{96}Y have been obtained from β-γ coincidences in the daughter port configuration. A γ-singles spectrum in a Ge detector and a β-singles spectrum in a β detector were concurrently

TABLE III. ^{96}Y→^{96}Zr Q_β values measured from individual β-γ spectra. All values are in keV.

γ transition	E_x^a	E_β^b	Q_β
469	2695	4433(80)	7128(80)
475	2226	4786(80)	7012(80)
1750	1750	5326(36)	7076(36)
2226	2226	4790(110)	7016(110)
5551	5551	1411(170)	6962(170)
			average=7067(30)

[a]Energy level deexcited by the gating γ transition.
[b]Includes a correction of 9.1(4) keV due to absorption in the entrance window of the β detector.

collected. The β decay was a hyperpure Ge detector in 10-mm active thickness with a 12-μm Ti window. Care was taken to keep the count rate below 2.5×10^3 sec^{-1} in each detector in order to minimize pileup effects which can severely distort the end-point energy determination. Approximately 2×10^7 β-γ-t coincidence triplets were collected on magnetic tapes and sorted offline. The β spectra in coincidence with selected γ rays were treated with a Fermi-Kurie analysis. The energy calibration was obtained offline using standard γ sources as well as internally using γ transitions present in the decay and high-energy neutron-capture γ lines which appear as contaminants in the singles β spectra. The correction for the energy loss in the windows, dead layers of the detector, etc., was determined from the energy shift of the intense 1581.4-keV K and L $E0$ conversion lines present in both the β singles and coincidence spectra.

Table III illustrates results of the Q_β measurements for the strongest gates in the ^{96}Y decay while Table IV presents a summary of the Q_β measurements. The β spectra gated by the 469-, 475-, 644-, 1750-, 2226-, 5551-, 5601-, and 5934-keV γ-ray lines confirmed (as expected from the properties of the γ-ray decay scheme, see Sec. III) that the levels at energies of 1750.4, 2225.7, 2695.2, 5551.4, 5601.3, and 5934.4 keV are predominantly fed by direct β feeding. On the other hand, the spectrum gated by the 918-keV line suggests that the main feeding of the 2668.9-keV level is by γ cascades.

The Q_β values deduced in the present work for the decays of ^{95,96}Sr and ^{96}Y compare very closely with the previous results[27–30] both when considered individually or as averaged. As an exception, we observe poor agreement with the Q_β value for the ^{96}Sr decay reported by Decker *et al.*[28] We further note that the Q_β values determined experimentally are systematically lower than the adjusted Q_β values in the compilation of Wapstra and Audi.[31]

TABLE IV. Comparison of the Q_β values from this and previous studies[27–30] and from the compilation of Wapstra and Audi.[31] All values are in keV.

Decay	Q_β This Work	Q_β Previous Measurements	Q_β Ref. 31
^{96}Sr→Y		5350(100)[a]	
		5413(20)[b]	
		5330(30)[c]	
	5354(40)	av=5386(20)	5416(20)
^{96}Y→Zr		7030(70)[a]	
		7120(50)[b]	
	7067(30)	av=7090(41)	7140(40)
^{95}Sr→Y		6060(100)[a]	
		6110(110)[d]	
	6052(25)	av=6083(74)	6120(60)

[a]Ref. 27.
[b]Ref. 28.
[c]Ref. 29.
[d]Ref. 30.

D. Absolute $E0$ and γ intensities

1. *Absolute $E0$ intensity from β-γ coincidences at the daughter port*

From the coincidence data described in the previous subsection, we have also extracted a γ-ray spectrum in coincidence with the 1581.4 K and L $E0$ conversion lines. A portion of this spectrum is shown in Fig. 2. The intensities (internally normalized to the strong 644- and 469-keV lines from the 2695→2226→1581 cascade) and energies of the coincident γ lines agree very well with those obtained in the GMS measurement, with the exception of the 4160-keV line, for which the intensity is much lower in the gated spectrum than in GMS singles thus indicating a doublet at that energy. Furthermore, we have used the coincidence data in combination with the γ- and β-singles to extract the absolute intensity of the 1581.4-keV $E0$ transition as described in the following.

The first-excited states in ^{96}Zr, ^{98}Zr, and ^{98}Mo are 0^+ states at 1581, 854, and 735 keV, respectively.[14,19,32] The latter two will decay to their ground states by $E0$ conversion while the ^{96}Zr 0_2^+ state, with $E_x>2m_0c^2$, decays by pair emission as well. For this level we calculate from Wilkinson[33] that $P_\pi/P_{e^-}=0.205$, where P_π and P_{e^-} are the probabilities per unit time for positron-electron pair emission and electron emission, respectively. The most distinct signals of the $E0$ transitions are the K and L $E0$ conversion peaks (See Fig. 6 of Ref. 14 for the $E0$ conversion spectrum of the $A=96$ decay chain.) In order to extract the absolute $E0$ intensity from these peaks we need to know the fraction of e^- conversion counts which they contain. This fraction can be determined from the β-γ coincidence spectrum as follows. Consider the schematic decay scheme of Fig. 3. For the events in coincidence with γ_1 we have a balance of feeding β rays and deexciting conversion electrons and electron-positron pairs:

$$I_{\beta_1}+I_{\beta_2}=I_{e^-}+I_\pi\ , \tag{1}$$

where the I are coincidence events per unit time for the indicated processes. Assume that the β detector is insensitive to γ rays and that it detects all β rays with equal efficiency. However, the fact that both e^- and e^+ are emitted in each pair emission must be taken into account. Thus the total number of counts per unit time in coincidence with γ_1 will be

$$I_T=I_{\beta_1}+I_{\beta_2}+I_{e^-}+2I_\pi=2I_{e^-}+3I_\pi\ . \tag{2}$$

If we now define f_s such that

$$\Sigma_{KL}=f_S\cdot I_{e^-}\ , \tag{3}$$

where Σ_{KL} is the coincidence counts per unit time in the full-energy K and L peaks of the $E0$ conversion, we have

$$f_S=2\frac{\Sigma_{KL}}{I_T}+(1+\tfrac{3}{2}[P_\pi/P_{e^-}])\ . \tag{4}$$

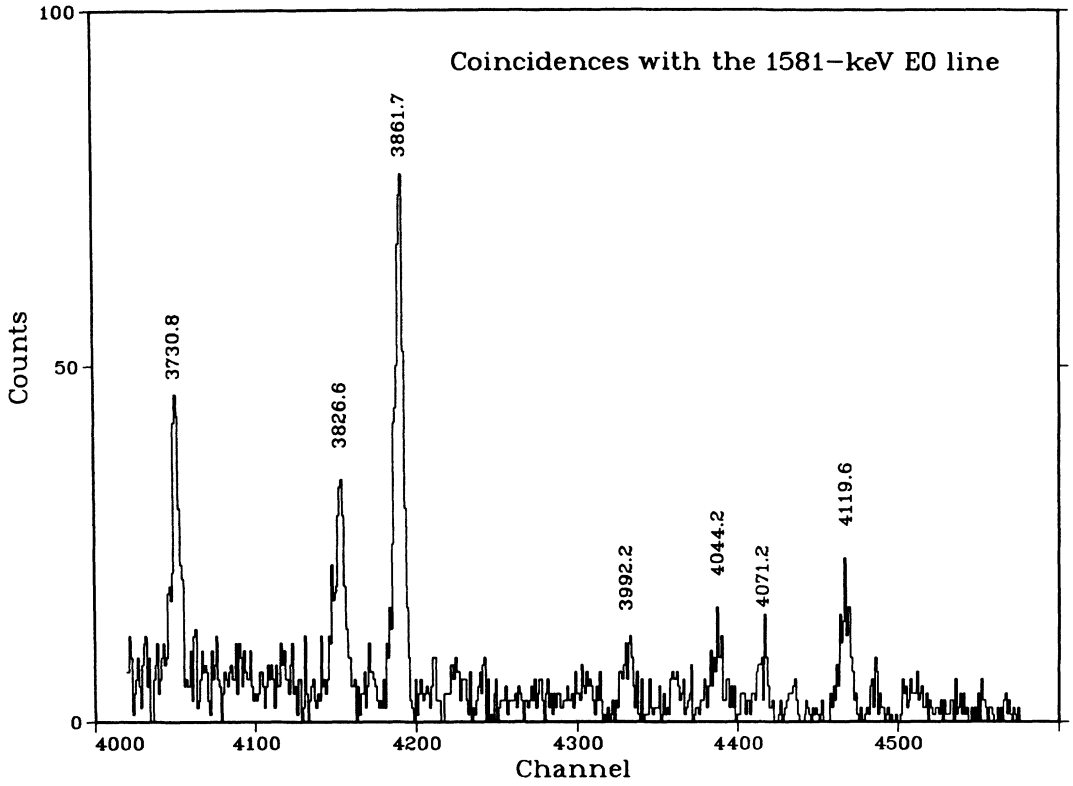

FIG. 2. A high-energy portion of the γ-ray spectrum in coincidence with the 1581-keV $E0$ transition indicating numerous but weak transitions feeding the 0_2^+ level.

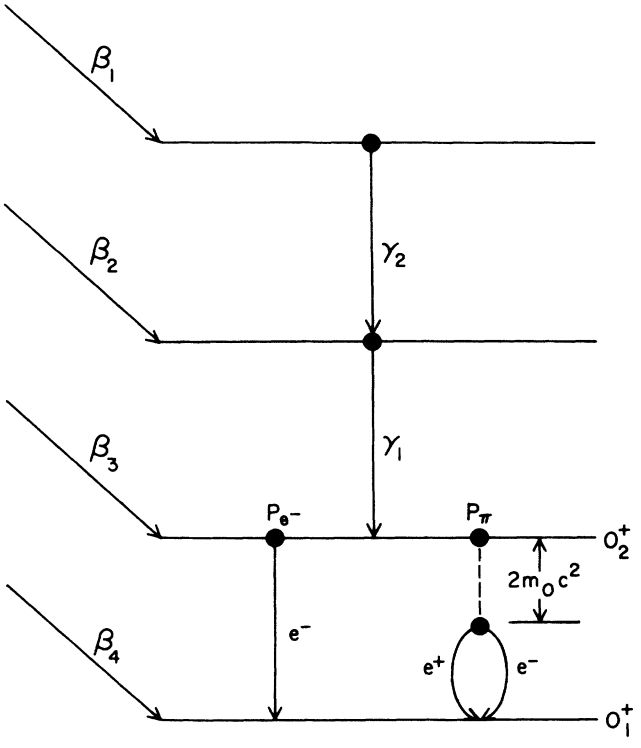

FIG. 3. Schematic illustrating the basis of the determination of the full-energy fraction, f_S, for an $E0$ transition via γ-β coincidences. The method is explained in the text.

To a good approximation the "thick" β detector used in this measurement fulfills the necessary conditions so that this method can be used to obtain f_S. Thus, from the coincident spectra gated by the 644-keV line in the decay of ^{96}Y, and from the gates of the 3310-keV (^{98}Y), and the 1024-keV (^{98}Nb) γ transitions from the $A=98$ decay chain (measured in a separate experiment), we obtained f_S values for the 1581-, 854-, and 735-keV $E0$ transitions. Using this result we extracted the total number of conversion electrons for the 1581-keV $E0$ transition in the singles β spectrum. Next, we obtained the total number of ^{96}Y β counts present in the β-singles spectrum by subtracting the impurity contributions such as conversion electron lines (0.1%), γ transitions (0.003%), one-half the pair counts for the 1581-keV transition (0.11%), the general background (estimated in the beam-off runs to be 7.5%), and betas from the β decay of ^{96}Rb, ^{96}Sr, and ^{95}Sr (10%) from the total number of counts. The latter were estimated from the relative intensities of the γ lines observed in γ-singles spectrum and the absolute intensities for those lines quoted in the literature.[19,24] For the absolute intensity of the 1750-keV γ-ray transition in ^{96}Zr we took the value of 2.35(24)% deduced in Sec. II D.2, below. Finally, from the ratio of the total number of 1581-keV $E0$ conversion electrons to the total number of betas associated with that decay and the calcu-

lated value of P_π/P_{e^-} we obtained the absolute intensity for the $E0$ line of 1.44(15)%.

2. *Absolute E0 and γ intensities from e^- and γ singles measurements at beam saturation*

We measured absolute $E0$ as well as γ intensities from the relative strength of conversion lines in an e^- spectrum and γ transitions in a γ-singles spectrum. Both spectra were obtained at the parent port with a saturated source, in which the beam was continuously collected and equilibrium was established among the decays in the $A=96$ isobaric chain. We used a specialized chamber in which the beam was dumped onto a thin Al foil in front of a thin plastic ΔE β detector, both tilted by about 45° to the direction of the beam. Conversion electron spectra were measured with a cooled 200-mm^2 Si(Li) detector that has a 2-mm depletion depth and a FWHM resolution of 1.4 keV at 624 keV. The electron detector, positioned at 90° to the beam direction, directly faced the beam deposition point, while a large volume Ge detector positioned on the opposite side viewed the deposition point through the thin plastic ΔE β detector. The energy and efficiency calibrations were measured offline using thin radioactive sources. We made simultaneous measurements of e^- and γ-singles spectra and e^--γ coincidences. We also measured e^- and γ-singles spectra gated by coincident signals from the ΔE β detector, which help to enhance the peak to background ratio for weak lines by reducing the continuous β-ray background and background γ radiation. Two sets of data were collected in separate runs lasting 18 and 32 h, respectively, in which different source-detector distances were used. Approximately 3×10^7 e^--γ-t coincident triplets were recorded and sorted off line.

The ratio of the peak area to the area of the total response function for monoenergetic electrons was deduced for the 854- and 735-keV $E0$ transitions in the $A=98$ mass chain using coincidence data collected in a separate run. These ratios were obtained according to the method described in the previous section and were used to construct a "peak efficiency curve." This curve is simply a relative conversion-electron peak efficiency measured offline using calibrated sources and renormalized to the 854- and 735-keV values. The coincidence spectra gated by the 122-, 279-, 530-, and 809-keV lines from the decay of ^{96}Sr and the 352-keV line in ^{95}Rb decay yielded composite spectra which consisted of beta continuum and conversion electron lines. Consequently, from the ratio of the total number of K-conversion electrons to the total number of corresponding betas, we have directly deduced the K-conversion coefficients for the 122-, 279-, and 530-keV lines in ^{96}Y and the 204-keV line in ^{95}Sr. No correction has been made for the expected low anisotropy of the β-γ and e^--γ angular correlations involved. The electron conversion coefficients deduced from the coincidence data agree to within the statistical uncertainties with those deduced from the analysis of the gated and ungated e^- and γ-singles spectra, and thus provide an important check of the procedures used.

From the β-singles spectrum we extracted the absolute intensities of the 1581-keV $E0$ K and L conversion lines in ^{96}Zr and the 815-keV $E2$ conversion lines in ^{96}Sr using a procedure similar to the one outlined in Sec. II D.1. The number of ^{96}Y$\rightarrow$^{96}Zr betas that were present in the total β-singles spectrum was deduced from the total number of counts in the spectrum by subtracting the contribution due to conversion electrons, gammas, and general background counts, and by dividing among participating $A=95$ (^{95}Rb$\rightarrow$^{95}Sr$\rightarrow$^{95}Y$\rightarrow$^{95}Zr) and $A=96$ (^{96}Rb$\rightarrow$^{96}Sr$\rightarrow$^{96}Y$\rightarrow$^{96}Zr) β decays using the ratio of 13.8:86.2 for the β-delayed neutron branch.[19] From the ratio of $E0$ counts to the ^{96}Y β counts we obtain the absolute intensity of the 1581-keV $E0$ decay (e^-+pairs) in ^{96}Zr as 1.36(20)%. This number compares well with the value of 1.44(15)% deduced in Sec. II D.1 leading to the average value of 1.41(12)% adopted in this study. In the previous TRISTAN study,[14] we obtained a value of 1.4(5)% which was deduced by a rather complex renormalization to the absolute γ intensities. This value, however, was not corrected for the contribution from the internal pair branch. The corrected value of 1.7(6)% remains in good agreement with the present value. In a parallel measurement, van Klinken and co-workers[34] deduced the absolute intensity for this $E0$ line as 0.5(2)% as an average of two values:[35] $I_{E_0}^{abs}=0.5(1)$% deduced at the OSTIS mass separator using a method similar to that of Ref. 14, and a second value of 0.34(15)% obtained from the conversion electron spectra of the fission products in the α-induced fusion-fission reaction on the ^{238}U target. We provide no explanation for the discrepancy of our result with the first value. On the other hand, the second value was obtained by normalizing the $E0$ conversion-line intensity to an absolute intensity of 5.5(11)% for the 735-keV $E0$ line in ^{98}Mo. The absolute intensity of the ^{98}Mo line has been recently remeasured[20] to be 26(6)%, thus higher than the previous values by a factor of $\sim$4.7. Using these latest results we renormalize the second set of van Klinken[35] results and obtain an absolute intensity for the 1581-keV $E0$ lines in ^{96}Zr of 1.6(7)% in agreement with our measurement.

In a similar manner, using the number of counts in the electron K peak of the composite 814-keV peak (due to the unresolved 813- and 815-keV lines from the decay of ^{96}Rb), the total number of corresponding β rays, and the $E2$ $\alpha_K=0.00\,087(3)$ coefficient, we deduce an absolute intensity for the 814-keV line of 78(7)% which compares very closely with the adopted value[17] of 83(3)%. Furthermore, using the number of counts in the K peak of the 809-keV transition in the decay of ^{96}Sr, the total number of corresponding β counts, and the $\alpha_K=0.00\,036(4)$ coefficient for that transition, we deduce the absolute intensity for the 809-keV line to be 79(11)% in agreement with the adopted value[17] of 71.9(26)%.

Next, we used the relative γ intensities in the γ-ray singles spectrum (obtained with a saturated source) to deduce the absolute intensity of the 1750-keV line in ^{96}Zr. First we deduced the absolute intensities of γ intensities from ^{96}Rb$\rightarrow$^{96}Sr and ^{96}Sr$\rightarrow$^{96}Y to test our method before using it to measure the absolute intensity of the 1750-keV line. The measurement yielded $I_\gamma=2.35(24)$% in good agreement with our previous result[14] of 2.9(9)%.

III. LEVEL SCHEME OF ^{96}Zr AND THE STRENGTH OF THE 0_1^- ^{96}Y$\rightarrow 0_1^+$ ^{96}Zr TRANSITION

The results of the present experimental investigation are summarized in Fig. 4 which illustrates a partial decay scheme for the 5.3 s ^{96}Y$\rightarrow^{96}$Zr isomer constructed from the data of Table II. The decay scheme is for $E_x < 5$ MeV. Information on levels with $E_x > 5$ MeV can be readily extracted from Table II. The sensitivity of the measurements is ~50 times that of the previous TRIS-

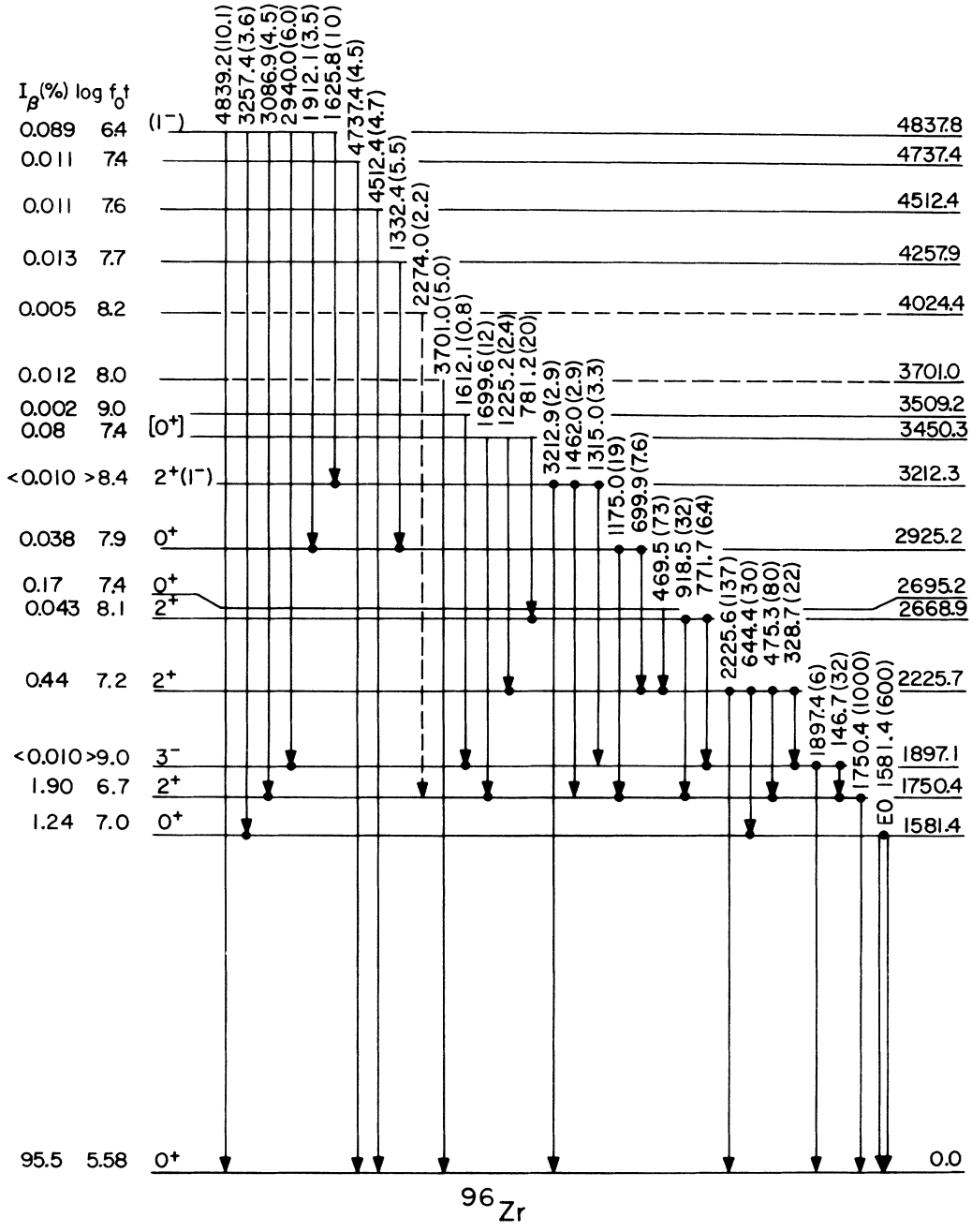

FIG. 4. A level scheme for the decay of the 5.3 s 0^- isomer of ^{96}Y to ^{96}Zr states below 4.9 MeV. With two exceptions, only levels fed in the β decay are included in the figure. Spin-parity assignments are from Refs. 14 and 36 except for the 3450- and 4838-keV levels which are based on the log f_0t values and γ-branching ratios observed in this work. Assignments that are not quite definite are enclosed in parentheses and speculations are in brackets. Gamma-ray transitions are identified by their energies (in keV) and their relative intensities (in parentheses). The β-feeding intensities, I_β, are calculated from the γ-ray intensities listed in Table II and shown in the figure. These I_β result in the listed logf_0t values.

TAN study.[14] Despite this, the agreement is excellent, and in particular only a summed β intensity of 0.6% was found to feed levels with $E_x > 4$ MeV. Only one energy level—at 4838 keV—was identified as most likely to be fed by an allowed transition. This level is given a most probable $J^\pi = 1^-$ assignment from the combination of its γ deexciting properties (it feeds levels of spin 0^+, 2^+, and 3^-) and from the $\log f_0 t$ value of 6.4. We note that this level is fed very weakly in β decay in comparison, e.g., to the strongly fed 1^- levels in $^{98}\mathrm{Y}(0^-) \rightarrow {}^{98}\mathrm{Zr}$ (Ref. 20); However, it is at a similar excitation energy and has a similar γ-ray deexcitation pattern.

In comparison to the previous TRISTAN study,[14] we report a number of new γ-ray transitions but found evidence for only one additional level below 3.5 MeV–the 3212-keV level that has also been observed in the $(n,n'\gamma)$ studies of Mölnar, *et al.*[36]. The γ-ray intensities of the two studies are in excellent agreement (due to a printing error, the intensity of the 699-keV line was mistakenly reported in Ref. 14 as 18 rather than as 8). We note at this point that the sensitivity of the γ-γ and $E0$-γ coincidence measurements requires that any ^{96}Y transition of energy $E_\gamma \leq 5.5$ MeV identified in the GMS spectrum must be observed in the coincidence gates unless the transition feeds the ground state directly. In addition, transitions of energy above 5.5 MeV must feed the ground state unconditionally, since feeding of any of the excited states would imply a new energy level at an excitation energy exceeding the Q_β value.

It is interesting to compare our β-decay results with the $(n,n'\gamma)$ and $(p,p'\gamma)$ measurements reported recently[36] on ^{96}Zr. Our observed γ-ray energies and branching ratios are in excellent agreement with these results. As regards the differences, the comparison should reveal new 0^+ states as these are the only low-spin states weakly populated in the compound—and thus otherwise highly unselective—(n,n') reaction. All the levels reported in the beta decay with $E_x < 4$ MeV are also observed in the study by Molnár *et al.*[36] with the exception of the 3450-keV level. It is thus suggested that the spin parity of the 3450-keV level, the existence of which is firmly established in our β-decay study, is most likely 0^+. The highly hindered β feeding of this level, $\log f_0 t = 7.4$, as well its γ-ray deexcitation pattern—feeding exclusively levels of spin 2^+—is consistent with this assignment. Note that there are no known 1^- levels below 3450 keV in ^{96}Zr.

Despite new and independent determinations of the crucial relative intensities of the 1750-keV γ-ray transition and the 1581-keV $E0$ transition, the ground-state feeding was found to be an almost identical to that quoted previously[14] (i.e., 95.5% vs 95.2%). The β feeding of the 0_2^+ level —1.24(11)%—is the same within errors as in the previous study. The feeding of the 2_1^+ level—1.90(20)%—is, however, slightly smaller than previously reported, in part due to the higher sensitivity of the measurement that helped to identify a large number of high-energy transitions feeding this state, and in part due to the lower absolute γ intensity reported in this study for the 1750-keV line. Thus this study does not indicate any major revision of the decay of the 5.3 s isomer of ^{96}Y but it provides a complete (rather than limited to $E_x < 4$ MeV) decay scheme with higher precision and a much improved confidence such that a meaningful comparison between the calculations and the data can be made. We now turn to such a comparison.

IV. SHELL-MODEL CALCULATIONS

A. The interaction

A proper shell-model study of $A = 96$ nuclei with emphasis on $^{96}\mathrm{Y}\ 0^- \rightarrow {}^{96}\mathrm{Zr}\ 0^+\ \beta^-$ decay necessitates the involvement, at a minimum, of the proton $0f_{7/2}$, $0f_{5/2}$, $1p_{3/2}$, $1p_{1/2}$, $0g_{9/2}$ shells and the neutron $0g_{7/2}$, $1d_{5/2}$, $1d_{3/2}$, and $2s_{1/2}$ shells. This allows the expected[9,10,17] destructive interference between the contributions from the possible j orbits which are governed by the $0^- \rightarrow 0^+$ selection rule $j_i = j_f$. The $0^- \rightarrow 0^+$ decay is shown schematically in Fig. 5. The dominant term in the transition will be $\nu 2s_{1/2} \rightarrow \pi 1p_{1/2}$, but a net destructive contribution is expected from the other three possible $\nu j \rightarrow \pi j$ transitions. The inclusion of the $\pi g_{9/2}$ shell is necessary because of the near degeneracy of the $\pi p_{1/2}$ and $\pi g_{9/2}$ shells. Another amplitude which will enter in first order and is expected to be important[6,10,11] is the $1p1h \rightarrow 2p2h$ term from $\nu(0f,1p) \rightarrow \pi(1d,2s)$ transitions and we would like to include an estimate of the effect of this amplitude as well. Initially, the two-body-matrix elements (TBME) of the nine subshells of the $(0f,1p)(0g,1d,2s)$ major shells were generated from the G-matrix potential of Hosaka, Kubo, and Toki.[37] It is expected that the single-particle energies, $\epsilon(j)$, of the proton orbits will be dependent on neutron number and *vice versa* so that it is desirable to fix them from consideration of nearby nuclei. Thus, when possible, the $\epsilon(j)$ were evaluated from experimental spectra of $A = 95$–97 nuclei. In particular, the relative $\epsilon(j)$ for the neutron $1d_{5/2}$ and $2s_{1/2}$ orbits were taken from the least-squares fit of Gloeckner,[38] and the $\epsilon(j)$ for the neutron $1d_{3/2}$ and $0g_{7/2}$ orbits were set so as to reproduce (roughly) the spectrum and spectroscopic factors of ^{97}Zr (Ref. 39). Likewise, the proton $\epsilon(j)$ were chosen so as to reproduce (roughly) the relative $^{96}\mathrm{Zr}\ 0_1^+$, $^{95}\mathrm{Y}\ \frac{1}{2}1^-, \frac{3}{2}1^-, \frac{5}{2}1^-, \frac{9}{2}1^+$ binding energies.[31,32] Of course, the $\epsilon(j)$ chosen depend on the model space used. These calculations were done in a fairly complicated model space. For the deeply bound proton $0f_{7/2}$ orbit, $\epsilon(j)$ was taken from a measurement for the splitting of the $\frac{1}{2}^-$ and $\frac{7}{2}^-$ spectroscopic pickup strengths in ^{89}Y of 6.8 MeV.[40] The $\epsilon(j)$ for the neutron $(0f,1p)$ orbits [proton $(1d,2s)$ orbits] were estimated by adding [subtracting] an average Coulomb energy from the corresponding proton [neutron] $\epsilon(j)$. most of our studies of ^{96}Y and ^{96}Zr were performed in a model space consisting of $0f_{7/2}$, $0f_{5/2}$, $1p_{3/2}$, $1p_{1/2}$, $0g_{9/2}$ proton orbits and $1d_{5/2}$, $2s_{1/2}$, $1d_{3/2}$, $0g_{7/2}$ neutron orbits. The G-matrix interaction for the full $(0f,1p)(0g,1d,2s)$ model space described here was used to verify that the results in this smaller model space were consistent with expectations based on general properties of the nucleon-nucleon interaction. It was also used to estimate the correction term due to $1p1h \rightarrow 2p2h$ ampli-

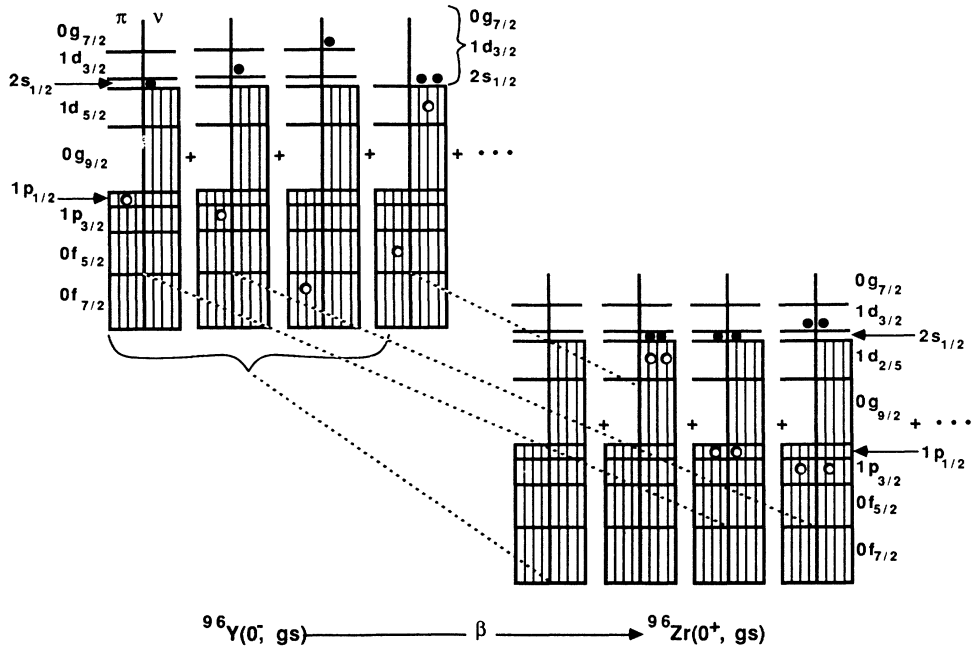

FIG. 5. Schematic showing leading terms and several of the possible $1\hbar\omega \rightarrow 2\hbar\omega$ terms in $^{96}Y^{g} \rightarrow {}^{96}Zr^{g}$ β^- decay.

tudes since these amplitudes are not possible in the smaller model space.

We now consider modifications to the G-matrix interaction in order to better describe nuclei in the $A=96$ region. The major components in the wave functions of the low-lying odd-parity levels of ^{96}Y and even-parity levels of ^{96}Zr arise from active participation of the $\pi(0p_{1/2},0g_{9/2})$ and $\nu(1d_{5/2},2s_{1/2})$ orbits since these orbits are closest to the Fermi surface. This is just the model space of the Gloeckner interaction,[38] accordingly, the TBME of the Gloeckner interaction[38] were adopted for those four orbits. This tunes the interaction to the experimental level schemes of the $Z=40$–41, $N=50$–56 nuclei considered by Gloeckner.[38] One further substitution was made. Ji and Wildenthal[41] performed a least squares fit to experimental level schemes for $Z=32$–46, $N=50$ nuclei assuming active $0f_{5/2}$, $1p_{3/2}$, $1p_{1/2}$, $0g_{9/2}$ orbits and a closed $0g_{9/2}$ neutron shell. This interaction gave a very successful accounting of known level schemes for $N=50$ nuclei in the region studied and we also adopt the appropriate 65 proton TBME. There is a possible conflict here since the Ji-Wildenthal and Gloeckner interactions both specify the nine proton $\pi(1p_{1/2},0g_{9/2})$ TBME. As noted by Ji and Wildenthal,[41] these two sets of TBME are practically identical so that there actually is no problem. We use the Gloeckner set. As before, the $\epsilon(j)$ were determined from experimental level schemes for $A=95$–97 nuclei.

A problem often encountered in shell-model calculations involving more than one major shell is how to determine—and, if possible, correct for—the degree of spuriosity, i.e., the contribution to the wave functions of center-of-mass motion of the nucleus. In most of these calculations the neutrons are confined to one major shell and the $1\hbar\omega$ excitation of the protons is from the $(0f,1p)$ shell to the $0g_{9/2}$ orbit with $\Delta j > 1$. Under these conditions, there is no spurious contribution.[42] The exceptions are in the estimation of the role of $2p2h$ terms and of the $0f_{7/2}$ orbit and since the contributions from these two sources are small the overall effect of any spuriosity will be also.

B. Definition of β transition strengths

We shall consider $0^- \rightarrow 2^+$ unique rank-two decays as well as $0^- \rightarrow 0^+$ rank-zero decays. Usually, there are six matrix elements which contribute non-negligibly to first-forbidden beta decay. Only one of these is of rank two and thus the $0^- \rightarrow 2^+$ decays are classified as unique with the matrix element separable from the integrated Fermi function. A simplification also results for $0^- \rightarrow 0^+$ decays since, to a good approximation, only allowed terms (i.e., terms in the shape factor that are independent of energy) contribute. In this case, for instance, this approximation is good to better than 4%. Thus, to this accuracy, we can define transition strengths $B_1^{(R)}$ for first-forbidden transitions of rank $R=0$ or 2 and write:[17]

$$B_1^{(0)} = \frac{6166 \text{ sec}}{f_0 t} \lambda\!\!\!^{-2}_{ce}; \quad B_1^{(2)} = \frac{3 \times 6166 \text{ sec}}{f_1 t} \lambda\!\!\!^{-2}_{ce}, \tag{5}$$

where $\lambda\!\!\!^{-}_{ce}$ is the Compton wavelength of the electron (386.159 fm), and f_0 and f_1 are Fermi integrals evaluated with shape factors of unity and $(q^2+\lambda^2 p^2)$, respectively, where λ is a Coulomb function[17] and q and p are the neutrino and electron momenta. There are two matrix elements contributing to $B_1^{(0)}$, the spacelike, M_0^S, and time-

TABLE V. Comparison of experimental first-forbidden β^- transition strengths in the decay of $^{96}Y^g(0^-)$ with extreme single-particle estimates (spe) and with calculation "C". All $B_1^{(R)}$ are in fm^2. For the $0^- \rightarrow 0^+$ transitions $\epsilon_{mec}=1.75$ [Eq. (6)].

State	Experiment		$a(Z,W_0,r)$	spe	Calc. "C"	
J_k^π	E_x(keV)	$B_1^{(R)}$		$B_1^{(R)}$	E_x(keV)	$B_1^{(R)}$
0_1^+	0	2424	12.69	3649	0	1211
0_2^+	1581	99	11.66	4376	1563	366
0_3^+	2695	38	10.94	4910	2737	31
2_1^+	1750	7		86	2294	0.2
2_2^+	2226	3		86	2876	1.8
2_3^+	2669	1		86	3576	27

like, M_0^T, components of the rank-zero axial current. The $R=0$ transition strength is given by[17]

$$B_1^{(0)}=[M_1^{(0)}]^2=[\epsilon_{mec}M_0^T+a(Z,W_0,r)M_0^S]^2 , \quad (6)$$

where we have defined M_0^T and M_0^S to be the free-nucleon (impulse approximation) values of the matrix elements and explicitly displayed the enhancement factor, ϵ_{mec}, due to meson exchange. Calculation of the constant $a(Z,W_0,r)$ is explained by Warburton *et al.*[17]

We evaluate the two rank-zero matrix elements and the rank-two matrix element with harmonic oscillator (HO) wave functions with $\hbar\omega=45A^{-1/3}-25A^{-2/3}$ MeV and length parameter $b=(41.467/\hbar\omega)^{1/2}$. For $A=96$ we have $\hbar\omega=8.635$ MeV and $b=2.191$ fm. With HO wave functions and transitions of the type $(n+1)\hbar\omega \rightarrow n\hbar\omega$ there is a simple relationship between M_0^S and M_0^T:

$$M_0^T=-\left[\frac{\hbar\omega}{m_e c^2}\right]M_0^S \equiv -E_{osc}M_0^S , \quad (7)$$

i.e., E_{osc} is the energy of an oscillating quantum ($\hbar\omega$) in units of m_e. This simple relationship is broken in two ways. First, if $(n+2)\hbar\omega$ components are included in the final state then the terms due to $(n+1)\hbar\omega \rightarrow (n+2)\hbar\omega$ transitions will be destructive in one matrix element and constructive in the other.[6,17] Second, the effect of deviations of the radial wave functions from the HO form are expected to be opposite in the two matrix elements.[10,17]

An orientation towards the expected $B_1^{(R)}$ values in $^{96}Y^g$ decay can be obtained through consideration of the simplest possible decays, namely

$$[\nu(1d_{5/2}^6 2s_{1/2})\pi(1p_{1/2}^{-1})]_{0^-} \xrightarrow{\beta^-} [\nu(1d_{5/2}^6)\pi(1p_{1/2}^2)]_{0^+} \quad (8a)$$

$$[\nu(1d_{5/2}^6 2s_{1/2})\pi(1p_{1/2}^{-1})]_{0^-} \xrightarrow{\beta^-} [\nu(1d_{5/2}^5 2s_{1/2})\pi(1p_{1/2}^2)]_{2^+} . \quad (8b)$$

For these we find

$$M_0^S[(1p_{1/2}^{-1}2s_{1/2})\rightarrow \text{vacuum}] = 2(C_A/C_V)b = 5.524 \text{ fm} , \quad (9a)$$

$$M_0^T=-E_{osc}M_0^S=-16.895M_0^S=-93.33 \text{ fm} , \quad (9b)$$

and

$$B_1^{(2)}=[3.345(C_A/C_V)b]^2=85.45 \text{ fm}^2 , \quad (9c)$$

where $C_A/C_V=1.2605$. The experimental $B_1^{(R)}$ values for the first three 0^+ and 2^+ states of ^{96}Zr are listed in Table V. The single-particle values of Eqs. (6)–(9) are also included in the table. The last column of Table V gives the results of the shell-model calculations that we now describe.

C. Shell-model results for the β^- transition strengths

The wave functions of $^{96}Y^g$ and the 0^+ and 2^+ states of ^{96}Zr were calculated for many degrees of complexity, i.e., combinations of active orbits. In order to describe the results clearly and succinctly, it is useful to introduce several symbols. First we shall speak of an hypothetical $Z=40$, $N=56$ core labeled $^{96}Zr^{(c)}$, composed of full proton shells up through $\pi 1p_{1/2}$ and full neutron shells up through $\nu 1d_{5/2}$. We shall specify excitations relative to this core and shall often drop components when they are unspecified or not excited. Secondly, we define a partition $\mathcal{P}$ as a specific combination of active orbits. Thus, a particular wave function will be composed, in general, of many partitions:

$$\mathcal{P}=[p(f_{7/2}),p(f_{5/2}),p(p_{3/2}),p(p_{1/2}),p(g_{9/2})|n(g_{7/2}),n(d_{5/2}),n(d_{3/2}),n(s_{1/2})] , \quad (10a)$$

where $p(j)$ and $n(j)$ are the number of protons and neutrons, respectively, in a particular orbit j. Another useful concept is the mean partition $\bar{\mathcal{P}}(J_k^\pi)$ given by

$$\bar{\mathcal{P}}(J_k^\pi)=[\bar{p}(f_{7/2}),\bar{p}(f_{5/2}),\bar{p}(p_{3/2}),\bar{p}(p_{1/2}),\bar{p}(g_{9/2})|\bar{n}(g_{7/2}),\bar{n}(d_{5/2}),\bar{n}(d_{3/2}),\bar{n}(s_{1/2})] , \quad (10b)$$

where $\bar{p}(j)$ and $\bar{n}(j)$ are the mean number of protons and neutrons, respectively, in orbit j for the state J_k^π. Results given in this notation are more easily absorbed if one remembers that the four $(0f,1p)$ subshells are followed by five $(0g,1d,2s)$ subshells, each in decreasing order of j.

We first consider a minimal calculation for 0^- ^{96}Y and 0^+ ^{96}Zr, i.e., one that contains the two components $^{96}\mathrm{Zr}^{(c)}$ and $^{96}\mathrm{Zr}^{(c)}\nu(1d_{5/2}^{-2}2s_{1/2}^2)$ in the ^{96}Zr 0_1^+ state and the four particle-hole partitions shown explicitly in Fig. 5 for the initial 0^- state. We also include an estimate of the $1\hbar\omega\rightarrow 2\hbar\omega$ term calculated with the G-matrix interaction (see Sec. IV A) and added perturbatively. (This term was calculated with $\nu 2s_{1/2}\pi 1p_{1/2}^{-1}$ and $\nu 1d_{3/2}\pi 1p_{3/2}^{-1}$ terms in the initial state and, for the final state, all possible combinations of the $j=\frac{1}{2}$ and $\frac{3}{2}$ orbits which connect to the initial state.) The results, summarized in Table VI, are much as expected. Each M_0^T term is given by $\pm E_{\mathrm{osc}}$ times the corresponding M_0^S term with the minus sign for the $1\hbar\omega\rightarrow 0\hbar\omega$ terms and the plus sign for the $1\hbar\omega\rightarrow 2\hbar\omega$ term. The simple $\nu 1d_{3/2}\pi 1p_{3/2}^{-1}$ and $\nu 0g_{7/2}\pi 0f_{7/2}^{-1}$ terms are in destructive interference with the main $\nu 2s_{1/2}\pi 1p_{1/2}^{-1}$ term. This destructive interference is expected from the repulsive nature of the $T=1$ part of the particle-hole interaction, a general property of nuclear matter. The $\nu 1d_{5/2}\pi 1f_{5/2}$ term is an exception because it actually arises from a $\nu 1d_{5/2}^{-1}2s_{1/2}^2$ component in the initial state so that more than a simple particle-hole interaction is involved.

For $\epsilon_{\mathrm{mec}}=1$ and $a(Z,W_0,r)=12.69$ (Table V), the minimal result gives a value for $M_1^{(0)}$ [Eq. (6)] of 6.65 fm as compared to 23.20 fm for a pure $\nu 2s_{1/2}\pi 1p_{1/2}^{-1}$ $\rightarrow$vacuum transition [from Eq. (9)]. The diminution is drastic but actually less than occurs in the similar $^{16}\mathrm{N}\rightarrow{}^{16}\mathrm{O}$ decay where, e.g., the effect of the $1\hbar\omega\rightarrow 2\hbar\omega$ term is considerably larger.[6,10] The effective interaction in nuclei scales roughly as $A^{-0.3}$ and the difference here between ^{16}O and ^{96}Zr appears to be due to this reduction in its strength as well as to the insulation of the $2\hbar\omega$ terms from the Fermi surface by the $0g_{9/2}$ shell. The result $M_1^{(0)}=6.65$ fm is far below the experimental value (see Table V) of $M_1^{(0)}=[B_1^{(0)}]^{1/2}=49.2$ fm and, although the calculated result for $\epsilon_{\mathrm{mec}}=1.0$ has a large uncertainty due to the high degree of cancellation between M_0^T and M_0^S, the argument for meson enhancement is seen to be compelling. The value of ϵ_{mec} needed to reproduce the experiment is 1.75, i.e., a meson enhancement for M_0^T of 75%.

So far we have not considered the errors introduced by using HO radial wave functions. This is a big effect near $A=16$ where HO wave functions are a relatively poor representation of realistic radial wave functions.[9,10] We examined this problem for a single-particle $\nu 2s_{1/2}\pi 1p_{1/2}^{-}\rightarrow$vacuum $^{96}\mathrm{Y}(0^-)\rightarrow{}^{96}\mathrm{Zr}(0^+)$ transition using both Woods-Saxon[43] and Hartree-Fock[44] radial wave functions. The root-mean-square nuclear radius was constrained to be the same in all cases, and unlike the $A=16$ region the three results for the single-particle matrix elements differed by less than 3% when globally chosen Woods-Saxon parameters[43] were used. The main reason for the smaller difference between the HO and WS results and an accompanying lessened sensitivity to the parameters of the WS potential—relative to $A=16$—is the larger neutron separation energy, 5.16 MeV, for ^{96}Y as opposed to, say, that for ^{16}N, 2.49 MeV. From an examination of the sensitivity of M_0^T and M_0^S to the radial wave functions we assume, throughout this study, a 7% uncertainty in M_0^T and M_0^S from this source. Since the uncertainties are anticorrelated the final effect is larger than 7%–20% for $M_1^{(0)}$ for the case of Table VI with $\epsilon_{\mathrm{mec}}=1.75$.

The minimal calculation might appear to be unrealistically simple. What is the effect of adding more degrees of freedom to the initial and final states? In order to answer this question, we tried many different combinations of partitions and also varied the $\epsilon(j)$. The J dimensions of the initial and final wave functions for the $1\hbar\omega\rightarrow 0\hbar\omega$ terms of Table VI were 9 and 2, respectively. We calculated the $0^-\rightarrow 0^+$ rate for J dimensions up to $\sim$2000 and $\sim$1000, respectively, and found several combinations of model space and $\epsilon(j)$ which gave "reasonable" agreement with the known properties of $A=95$–97 nuclei. The relative values of the four $1\hbar\omega\rightarrow 0\hbar\omega$ terms of Table VI were found to be exceedingly stable against changes in the wave functions. In general, introducing complexity into the wave functions reduced the final value of $M_1^{(0)}$. From this study we conclude that 1.75 is the minimum value we extract for ϵ_{mec}. We also consider it to be the best value. This is so because, in all cases, adding complexity to the wave functions spreads more $M_1^{(0)}$ strength to higher-lying 0^+ levels than is observed experimentally. We illustrate this by the calculated results labeled calculation "C" (calc. "C") in Table V. These results use $\epsilon_{\mathrm{mec}}=1.75$ and a model space consisting of the partitions [7-8,5-6,3-4,0-2,0-2|0-1,4-6,0-1,0-2] for $^{96}\mathrm{Y}^g(0^-)$, and the 52 most energetically favored—by a simple accounting of the $\epsilon(j)$—partitions in the set [8,4-6,2-4,0-2,0-4|0-2,2-

TABLE VI. Contributions to $M_1^{(0)}$ for the calculation with the minimal model space. The matrix elements M_0^S and M_0^T are in fm. For $\epsilon_{\mathrm{mec}}=1.75$ the matrix elements combine to give $B_1^{(0)}=2400$ fm^2, i.e., the experimental value.

	Configuration					
	$\nu s_{1/2}\pi p_{1/2}^{-1}$	$\nu d_{3/2}\pi p_{3/2}^{-1}$	$\nu d_{5/2}^{-1}\pi f_{5/2}^{-1}$	$\nu g_{7/2}\pi f_{7/2}^{-1}$	$2\hbar\omega$	Total
M_0^S	+5.13	−1.39	+0.17	−0.36	+0.28	3.83
M_0^T	−86.67	+23.48	−2.87	+6.08	+4.73	−55.25

6,0-2,0-2] for $^{96}Zr^{g}(0^+)$. Here 0–2, e.g., means all possible occupancies of 0, 1, or 2 nucleons in the specified orbit [see Eq. (10a)].

As seen in Table V, calculation "*C*" gives too large a value for the $B_1^{(0)}$ of 0_2^+. This was the case for all our calculations. The very noticeable concentration of the experimental $0^- \rightarrow 0^+$ strength in the ^{96}Zr ground state was previously used as an argument[14] that the 0_1^+ state is an unusually pure $^{96}Zr^{(c)}$ state, $^{96}Y^{g}$ is a simple $1\hbar\omega$ $\nu 2s_{1/2}\pi 1p_{1/2}^{-1}$ excitation of 0_1^+, and 0_2^+ is mainly composed of $\pi 1p_{1/2}^2 \rightarrow \pi 0g_{9/2}^2$ excitations of 0_1^+ with probable neutron excitations also. Our calculations indicate a different picture. We do find the ^{96}Y 0_1^- state is a relatively pure $\nu 2s_{1/2}\pi 1p_{1/2}^{-1}$ state—for calculation "*C*" this component is 87%. However the wave functions of the ^{96}Zr 0^+ states are quite complex. In calculation "*C*" the $\bar{\mathcal{P}}(J_k^{\pi})$ for the first two 0^+ states are

$$\bar{\mathcal{P}}(0_1^+)=[8,5.9,3.7,1.8,0.6|0.0,5.5,0.1,0.4] \quad (11a)$$

$$\bar{\mathcal{P}}(0_2^+)=[8,5.2,3.8,1.2,1.8|0.0,5.0,0.1,0.9] . \quad (11b)$$

The 0_1^+ state does not have a large $\pi 1p_{1/2}$ occupancy but the other orbits are relatively active so that the state is only 58% $^{96}Zr^{(c)}$. Note, in particular, the strong participation of $\pi 1f_{5/2}$ and $\nu 2s_{1/2}$ in 0_2^+. These wave functions will be discussed further in the next subsection.

The calculated $0_1^- \rightarrow 0_2^+$ matrix elements are quite small—as are the experimental values—and thus are quite uncertain. From previous experience, we think it likely that only small changes in the effective interaction would be necessary in order to diminish the rate for 0_2^+ to the experimental value.

As seen in Table V, calculation "*C*" gives 0^+ excitation energies in excellent agreement with experiment, but too small a value of $M_1^{(0)}$ for 0_1^+ using $\epsilon_{\rm mec}=1.75$. A value of $\epsilon_{\rm mec}=2.08$ is necessary to give agreement. However, some of the other "reasonable" combinations of model space and $\epsilon(j)$ we considered gave adequate agreement with experiment for $\epsilon_{\rm mec}\approx 1.7$.

Calculation "*C*" is also seen to do poorly for the excitation energies and $B_1^{(2)}$ values for the 2^+ states. Again, some of the other "reasonable" calculations did better. In any case, the experimental $B_1^{(2)}$ values are very small and so accurate predictions are not expected. All "reasonable" calculations placed the $2s_{1/2} \rightarrow 1d_{5/2}$ strength of Eqs. (8b) and (9c) at $\sim$3.5-MeV excitation. The example shown of calculation "*C*" has the serious weakness of placing much of this strength in 2_3^+ whereas experimentally it must be in 2_k^+ states with $k>3$. The latter placement was found for some of the other "reasonable" calculations.

We conclude this subsection with a short summary of our findings *viz-a-viz* the value of $\epsilon_{\rm mec}$. Our best value is $\epsilon_{\rm mec}=1.75$. We assign an anticorrelated uncertainty of 7% to M_0^T and M_0^S due to possible variations in the radial wave functions. We also assign a correlated uncertainty of 20% to each due to uncertainties in the calculation of the $1\hbar\omega \rightarrow 0\hbar\omega$ terms and possible effects in such terms from contributions from outside our model space—such as, e.g., $0\nu h_{9/2}\pi 1p_{1/2}^{-2}0g_{1/2} \rightarrow \pi 1p_{1/2}^{-2}0g_{9/2}^2$ (Ref. 45). The estimation of the $1\hbar\omega \rightarrow 2\hbar\omega$ terms is assigned an anticorrelated uncertainty of 100%. When these uncertainties are folded together, we find $\epsilon_{\rm mec}=1.75\pm0.30$ as our best estimate of the meson enhancement and its uncertainty.

D. An examination of the role of the $\nu g_{7/2}$ orbit in $A=96-100$ 0^+ states

In 1979, Federman and Pittel[46] presented a unified shell-model description of nuclear deformation throughout the periodic table. In this seminal paper they summarized clearly the information and concepts showing that nuclear deformation can be understood as arising from the isoscalar component of the neutron-proton interaction and they emphasized the role of the relatively strong interaction which occurs when the neutrons and protons occupy the two orbits of a spin-orbit doublet.[47] They gave, as a specific example, a discussion of a shell-model calculation for ^{96,98,100}Zr where the $\nu 0g_{7/2},\pi 0g_{9/2}$ interaction is at play. The model space used in this example had an inert ^{94}Sr core, with the valence neutrons and protons restricted to the $\nu(2s_{1/2},1d_{3/2},0g_{7/2})$ and $\pi(1p_{1/2},0g_{9/2},1d_{5/2})$ orbits, respectively. Their interest was in tracing the onset of deformation as neutron pairs are added to an essentially spherical ^{96}Zr. They found the 0_1^+ state to be $\sim$80% $\pi 1p_{1/2}^2$ and the 0_2^+ state—experimentally at 1582 keV—to be $\sim$80% $\pi 0g_{9/2}^2$. As neutron pairs are added to ^{96}Zr, the effect of raising the Fermi surface is dramatic. They found a substantial occupation of the $\nu 0g_{7/2}$ orbit and an associated deformation due to the strong $\nu 0g_{7/2}\pi 0g_{9/2}$ interaction. In ^{98}Zr the 0_2^+ state comes down to 854 keV (experimentally) and it is found to be dominated by a highly coherent $\nu 0g_{7/2}^2\pi 0g_{9/2}^2$ coupling; while the ground state is still largely $\pi 1p_{1/2}^2$ (neutron orbit unspecified). When two more neutrons are added to produce ^{100}Zr, the Fermi surface rises to the close-lying $\nu 1d_{3/2}$, $0g_{7/2}$ orbits and the 0^+ ground state is now dominated by a $\nu 0g_{7/2}^2\pi 0g_{9/2}^2$ coupling.

Although all the functions we have considered were quite complex with many partitions contributing, we find substantial agreement with the Federman-Pittel results when we repeat the calculation in our expanded model space. The main differences involve ^{96}Zr where we now have active rather than inert neutrons. For ^{96}Zr the $\nu 2s_{1/2}$ shell is available and the $\nu 0g_{7/2}$ shell is rather removed from the Fermi surface. To summarize briefly, the ^{96}Zr 0_1^+ state in calculation "*C*" is composed predominantly (58%) of $^{96}Zr^{(c)}$, while the largest component (21%) for the 0_2^+ state is generated by the simultaneous promotion, from $^{96}Zr^{(c)}$, of both proton and neutron pairs: $\pi 1p_{1/2}^2 \rightarrow \pi 0g_{9/2}^2$ and $\nu 1d_{5/2}^2 \rightarrow \nu 2s_{1/2}^2$. The resulting $\bar{\mathcal{P}}(0_k^+)$ are given in Eqs. (11). We find that in ^{96}Zr the $\nu 0g_{7/2}$ shell is of little importance below $E_x\sim 5$ MeV where a state appears which is $\sim$80% composed of a $\nu 0g_{7/2}^2\pi 0g_{9/2}^2$ coupling with various partitions for the remaining orbits. Recall that Federman and Pittel assumed inactive neutrons for ^{96}Zr. It is worth emphasizing that because of the small energy gap between the $\pi 1p_{1/2}$ and $\pi 0g_{9/2}$ orbits on the one hand and the $\nu 1d_{5/2}$ and $\nu 2s_{1/2}$ orbits on the other, the wave functions of the

0_1^+ and 0_2^+ states differ in degree and not in kind. Thus, on the basis of the shell-model calculations we find it meaningless to speak of "intruder" states as arising from the promotion of nucleons across the hypothetical $^{96}Zr^{(c)}$ core.

For ^{98}Zr and ^{100}Zr our results—obtained with the same $\epsilon(j)$ as for the $A=96$ calculations—are again very similar to those of Federman and Pittel. We find the ^{98}Zr ground state to be largely composed of $\pi 1p_{1/2}$ pairs while the 0_2^+ state comes at ~ 1.2 MeV and is dominated by wave function components with $\nu 0g_{7/2}^2 \pi 0g_{9/2}^2$ terms (65%). For ^{100}Zr, the 0^+ ground state is now a highly coherent $\nu 0g_{7/2}^2 \pi 0g_{9/2}^2$ state while the 0_2^+ state is largely (88%) $\nu(0g_{7/2}^4 1d_{5/2}^{-2})\pi 0g_{9/2}^2$ with the $\nu 2s_{1/2}$ orbit full. Recent experiments lend support to these findings. Evidence for a predominant $\pi 1p_{1/2}^2$ structure for $^{98}Zr^g$ comes from an observation for the first-forbidden $^{98}Y^g(0^-) \rightarrow {}^{98}Zr^g(0^+)$ decay of $\log f_0 t = 5.8$ (Ref. 22). Such a small value is most easily understood with a large $\nu 2s_{1/2}$ component for ^{98}Y and a large $\pi 1p_{1/2}^2$ component for ^{98}Zr. Likewise, new lifetime measurements for the ^{100}Zr 0_2^+ and 2_1^+ levels[48] indicate a stronger deformation of 0_1^+ than previously found and an unusually weak mixing of the lowest two 0^+ states.

The preference for occupancy of the $\nu 2s_{1/2}$ orbit at the expense of the $\nu 1d_{5/2}$ orbit [see also Eq. (11)], is the most noticeable difference between our results and those of Federman and Pittel. (They assumed an inert full $\nu 1d_{5/2}$ shell and so once more the results are not necessarily in conflict.) The importance of $\nu 0g_{7/2}^4$ terms in ^{100}Zr suggests that a proper shell-model treatment of this nucleus might demand four nucleons in both the $\nu 0g_{7/2}$ and $\pi 0g_{9/2}$ orbits. That is, such terms might be necessary in order to fully describe the collectivity which has arisen due to the complete realization of the notions espoused by Federman and Pittel. Unfortunately, we cannot carry out such a calculation since the resulting dimensions are beyond our computational resources.

The transition from a spherical ^{96}Zr to a deformed ^{100}Zr has also been considered by Nazarewicz and Werner using the mean-field approach.[49] Their predictions are in accord with ours if we equate our lowest $\nu 0g_{7/2}^2$ excitation with their deformed 0^+ bandhead. In particular, they expect the deformed 0^+ band in ^{96}Zr to commence at 3.5–5 MeV as compared to our prediction of ~ 5 MeV.[50] The main difference in our results is that they include the $h_{11/2}$ orbit in their calculations and find it has a sizable effect in ^{98}Zr and ^{100}Zr. However, for the even-parity states below 3.5 MeV in ^{96}Zr the $h_{11/2}$ orbit will have even less effect than the $g_{7/2}$ orbit.

V. DISCUSSION OF THE SHELL-MODEL RESULTS

A. General considerations

The great success of the shell model in light nuclei ($A<40$) has been due in part to the large energy gap between major shells. For example, the lowest $\frac{5}{2}^+$ state in ^{15}N is at 5.27 MeV and the first $\frac{7}{2}^-$ state in ^{39}K is at 2.81 MeV. Thus, to a good approximation, the $0p$ shell and the $(0d,1s)$ shells can be treated as separate, complete entities. In contrast, the first $\frac{9}{2}^+$ state in ^{95}Y is 1.09 MeV above the $\frac{1}{2}^-$ ground state. Thus, a successful shell-model treatment of ^{96}Zr involves at least parts—and ideally all—of the $\pi(0f,1p)$, $\pi(0g,1d,2s)$, and $\nu(0g,1d,2s)$ shells. So far we have attempted only a caricature of the "ideal" model space because we have omitted some of the subshells and severely limited the occupancies of the remaining ones. Nevertheless, some interesting results have been obtained. We find the 0^+ states to have quite complex wave functions with the participation of many subshells. With calculation "C", we find C^2S values for proton pickup leading to the ^{97}Nb $J^\pi = \frac{1}{2}^-, \frac{3}{2}^-, \frac{5}{2}^-$, and $\frac{9}{2}^+$ states of 0.09, 0.00, 0.01, and 0.87 as compared to experimental values[39] of 0.14, 0.07, (0.01), and 0.88, respectively. Previously, the small proton spectroscopic factor found for the $^{96}Zr+p \rightarrow {}^{97}Nb(\frac{1}{2}^-)$ stripping reaction has been interpreted as evidence for a $^{96}Zr^{(c)}$ wave function for the ^{96}Zr ground state. The rather good agreement with experiment of calculation "C" for the $\frac{1}{2}^-$ and $\frac{9}{2}^+$ states is a clear reminder that this interpretation does not necessarily follow; if our calculation is to be believed, then this interpretation does not follow. The same general argument applies to the first-forbidden $^{96}Y^g \rightarrow {}^{96}Zr^g$ rate. The large transition strength for $^{96}Y(0_1^-) \rightarrow {}^{96}Zr(0_1^+)$ tells us that $^{96}Y(0_1^-)$ resembles $\mathcal{O}_{\beta^-}|^{96}Zr(0_1^+)\rangle$, where $\mathcal{O}_{\beta^-}$ is the first-forbidden β^- operator. It does not directly specify either the initial or final state.

The very rapid increase in the participation of the $\nu 0g_{7/2}$ subshell as neutron pairs are added to ^{96}Zr is a fascinating phenomena. By considering more active orbits, we have extended the original study of Federan and Pittel[46] and have substantiated their findings in general while adding more detail. In particular, we find essentially no participation of the $\nu 0g_{7/2}$ subshell below 5 MeV in ^{96}Zr. Although the $\nu h_{11/2}$ orbit was not included in our model space, we would expect the same nonparticipation of this orbit in ^{96}Zr as well. This expectation follows because we find that it is mainly the proximity to the Fermi surface that allows participation of a specific orbit so we expect the same general behavior with neutron number for $\nu h_{11/2}$ as for $\nu g_{7/2}$ but at a somewhat higher neutron number.

It has been postulated that the 0_2^+ state of ^{96}Zr is an excitation of both a neutron and proton pair relative to ^{96}Zr (see, e.g., Ref. 14). Indeed, in our calculations $^{96}Zr^{(c)}\pi(1p_{1/2}^{-2}0g_{9/2}^2)\nu(1d_{5/2}^{-2}2s_{1/2}^2)$ is the biggest component (21%) in the wave function, however, this component is not large enough to clearly characterize the state.

B. 0^- $^{96}Y \rightarrow 0^+$ ^{96}Zr decay

In our study of this decay we emphasized the concept of specificity;[51] namely a simple calculation was performed in which only wave function components that contribute directly to the specific process in question (β^- decay) were retained; in this case, this mainly means om-

itting the $0g_{9/2}$ shell from consideration in the minimal model space calculation of Table VI. Since it does not contribute directly to the β^- decay process, the major effect of including the $0g_{9/2}$ shell is to spread the decay strength to other 0^+ states as shown in Table V for calculation "*C*". We find our calculation overdoes this sharing of the strength (thus reducing our confidence in the calculation). However, we note that the effect is to diminish the calculated rate for $0_1^- \rightarrow 0_1^+$ even further below experiment than the minimal calculation and thus the case for meson enhancement is not weakened by this deficiency. We find a meson enhancement of $(75\pm30)\%$ compared to the recent direct calculation of 45% by Kirchbach and Reinhardt.[8] Clearly, the $0^{-96}\mathrm{Y} \rightarrow 0^{+96}\mathrm{Zr}$ first-forbidden decay has added evidence for meson enhancement of the time-like component of the axial current A_0. Further study is certainly desirable. A major goal should be a better shell-model interaction. If an interaction could be obtained which reproduced the spectroscopy of the $A=96$ region satisfactorily and gave a better representation of *both* the $0_1^- \rightarrow 0_1^+$ and $0_1^+ \rightarrow 0_2^+$ rates, then we certainly would have an increased confidence in the resulting magnitude of the meson enhancement.

ACKNOWLEDGMENTS

We thank A. Wolf for assistance during the experiment, D. J. Millener, W. Nazarewicz, and G. Molnár for valuable and stimulating discussions, and D. W. O. Rogers for providing results of Monte Carlo efficiency calculations. Research supported by the U.S. Department of Energy under Contract Nos. DE-AC02-76CH00016 and DE-AC02-79ER10493, and with the University of California (Lawrence Livermore National Laboratory) under contract No. W-7405-Eng-48, and in part by National Science Foundation (NSF) Grant No. PHY-87-14432 [Michigan State University (MSU)]. One of us (E.K.W.) is grateful for an Alexander von Humboldt–Stiftung which supported that part of the research carried out at Heidelberg University and the Max Planck Institute.

*Present address: IRS, National Research Council, Ottawa, K1A 0R6 Canada.

†Permanent address: Brookhaven National Laboratory, Upton, NY 11973.

[1]K. Kubodera, J. Delorme, and M. Rho, Phys. Rev. Lett. **40**, 755 (1978).

[2]M. Rho and G. E. Brown, Commun. Nucl. Part. Phys. A **10**, 201 (1981).

[3]P. Guichon and C. Samour, Nucl. Phys. **A382**, 461 (1982).

[4]M. Kirchbach and E. Truhlik, Fiz. Elem. Chastits At. Yadra **17**, 224 (1986) [Sov. J. Part. Nucl. **17**, 93 (1986)].

[5]M. Kirchbach, in *Proceedings of the International Symposium on Modern Developments in Nuclear Physics, Novosibirsk, 1987,* edited by O. P. Sushkov (World-Scientific, Singapore, 1987), p. 475.

[6]I. S. Towner and F. C. Khanna, Nucl. Phys. **A372**, 331 (1981).

[7]H.-U. Jäger, M. Kirchbach, and E. Truhlik, Nucl. Phys. **A404**, 456 (1983).

[8]M. Kirchbach and H. Reinhardt, Phys. Lett. **208B**, 79 (1988).

[9]D. J. Millener and E. L. Warburton, in *Proceedings of the International Symposium on Nuclear Shell Models,* edited by M. Vallieres and B. H. Wildenthal (World-Scientific, Singapore, 1985), p. 365.

[10]E. K. Warburton, *Interactions and Structures in Nuclei,* edited by R. J. Blin-Stoyle and W. D. Hamilton (Hilger, Bristol, 1988), p. 81.

[11]I. S. Towner, Annu. Rev. Nucl. Part. Sci. **36**, 115 (1986).

[12]M. Kirchbach, H.-U. Jäger, and M. Gmitro, Z. Phys. A **320**, 689 (1985).

[13]R. U. Khafizov, Phys. Lett. **162B**, 21 (1985).

[14]H. Mach, G. Molnár, S. W. Yates, R. L. Gill, A. Aprahamian, and R. A. Meyer, Phys. Rev. C **37**, 245 (1987).

[15]S. Raman and N. B. Gove, Phys. Rev. C **7**, 1995 (1973).

[16]There is also the A dependence of the mec to consider. This has been a concern of Kirchbach and collaborators (Ref. 7) who calculated the two-body meson contribution in $A=16$, 96, and 206. They find that the enhancement decreases somewhat with A (10% less in $A=96$ than in $A=16$).

[17]E. K. Warburton, J. A. Becker, B. A. Brown, and D. J. Millener, Ann. Phys. (N.Y.) **187**, 471 (1988).

[18]G. Sadler, T. A. Khan, K. Sistemich, J. W. Grüter, H. Lawin, W. D. Lauppe, H. A. Selić, M. Shaanan, F. Schussler, J. Blachot, E. Monnand, G. Bailleul, J. P. Bocquet, B. Pfeiffer, H. Schrader, and B. Fogelberg, Nucl. Phys. **A252**, 365 (1975).

[19]H.-W. Mueller, Nucl. Data Sheets **35**, 281 (1982) ($A=96$).

[20]H. Mach and R. L. Gill, Phys. Rev. C **36**, 2721 (1987).

[21]J. A. Becker, E. K. Warburton, and B. A. Brown, Lawrence Livermore National Labortory Report No. UCRL-96971, 1987 (unpublished).

[22]H. Mach, E. K. Warburton, R. L. Gill, R. F. Casten, A. Wolf, Z. Berant, J. A. Winger, K. Sistemich, G. Molnár, and S. W. Yates, *Nuclear Structure of the Zirconium Region,* edited by J. Eberth, R. A. Meyer, and K. Sistemich (Springer-Verlag, Berlin, 1988), p. 391.

[23]A. Piotrowski, R. L. Gill, and D. C. McDonald, Nucl. Instrum. Methods **224**, 1 (1984).

[24]P. Luksch, Nucl. Data Sheets **38**, 1 (1983) ($A=95$).

[25]D. W. O. Rogers, Nucl. Instrum. Methods **199**, 531 (1982).

[26]W. R. Nelson, H. Hirayama, and D. W. O. Rogers, Stanford Linear Accelerator Center Report No. SLAC-265, 1985.

[27]R. Stippler, F. Münnich, H. Schrader, J. P. Bocquet, M. Asghar, G. Siegert, R. Decker, B. Pfeiffer, H. Wollnik, E. Monnand, and F. Schussler, Z. Phys. A **284**, 95 (1978).

[28]R. Decker, K. D. Wünsch, H. Wollnik, E. Koglin, G. Siegert, and G. Jung, Z. Phys. A **294**, 35 (1980).

[29]P. Peuser, H. Otto, M. Kaffrell, G. Nyman, and E. Roekcl, Nucl. Phys. **A332**, 95 (1979).

[30]M. I. Macias-Marques, R. Foucher, M. Cailliau, and J. Belhassen, in Proceedings of the International Conference on Nuclei far from the Region of Beta-Stability, Leysin, 1970 (CERN Report 70-30, 1970).

[31]A. H. Wapstra and G. Audi, Nucl. Phys. **A432**, 1 (1985).

[32]H.-W. Müller, Nucl. Data Sheets **39**, 467 (1983) ($A=98$).

[33]D. H. Wilkinson, Nucl. Instrum. Methods **82**, 122 (1970).

[34]J. van Klinken, J. F. W. Jansen, W. Z. Venema, and B. Pfeiffer, *Nuclear Structure, Reactions, and Symmetries,* edited by R. A. Meyer and V. Paar (World-Scientific, Singapore, 1986), p. 665.

[35]J. van Klinken (private communication).

[36]G. Molnár, T. Belgya, B. Fazekas, Á. Veres, S. W. Yates, E. W. Kleppinger, R. A. Gatenby, R. Julin, J. Kumpulainen, A. Passoja, and E. Verho, Nucl. Phys. **A500**, 43 (1989).

[37]A. Hosaka, K.-I. Kubo, and H. Toki, Nucl. Phys. **A244**, 76 (1985).
[38]D. H. Gloeckner, Nucl. Phys. **A253**, 301 (1975).
[39]B. Haesner and P. Luksch, Nucl. Data Sheets **46**, 607 (1985) ($A=97$).
[40]A. Stuirbrink, G. J. Wagner, K. T. Knöpfle, L. K. Pao, G. Mairle, H. Riedesel, and K. Schindler, Z. Phys. A **297**, 307 (1980).
[41]X. Ji and B. H. Wildenthal, Phys. Rev. C **37**, 1256 (1988).
[42]P. J. Brussard and P. W. M. Glaudemans, *Shell-Model Applications in Nuclear Spectroscopy* (North-Holland, Amsterdam, 1977).
[43]J. Streets, B. A. Brown, and P. E. Hodgson, J. Phys. G **8**, 839 (1982).
[44]B. A. Brown, C. R. Bronk, and P. E. Hodgson, J. Phys. G **10**, 1683 (1984).
[45]Actually this particular term was estimated perturbatively using the G-matrix potential (Ref. 37). We find an $\sim 1\%$ constructive contribution to the 0_1^+ rate.
[46]P. Federman and S. Pittel, Phys. Rev. C **20**, 820 (1979).
[47]A. DeShalit and M. Goldhaber, Phys. Rev. **92**, 1211 (1953).
[48]H. Mach, M. Moszyński, R. L. Gill, F. K. Wohn, J. A. Winger, J. C. Hill, G. Molnár, and K. Sistemich, Phys. Lett. **B230**, 21 (1989).
[49]W. Nazarewicz and T. Werner, *Nuclear Structure of the Zirconium Region,* edited by J. Eberth, R. A. Meyer, and K. Sistemich (Springer-Verlag, Berlin, 1988), p. 277.
[50]W. Nazarewicz (private communication).
[51]A. Bohr and B. R. Mottelson, *Nuclear Structure* (Benjamin, Reading, Mass., 1975), Vol. 2.